

# Transport of Fluid and Current in Nanofluidic Channels: Importance of the Electrical Double Layer Thickness

[Dimitar N. Petsev](#), [Zhen Yuan](#) and [Gabriel P. Lopez](#), *University of New Mexico, Albuquerque, NM, USA*

## Abstract

The flow of fluids (pure liquids and solutions) in very narrow channels enjoys a substantial attention with the rapid development of the fields of micro and nanofluidics. Miniaturized integrated fluidic devices have a great potential for enhanced separation and analysis by reducing the required time and the sizes of the samples. In channels of submicron dimension the electrokinetic phenomena play a particularly important role since the electric double layers formed at the walls can occupy a substantial part of the channel volume. In our work we present a concise theory that allows obtaining analytical expressions for the transport of fluid (electroosmotic flow), ions (electric current) and dissolved charged molecules (analytes) in the case of a weak double layer overlap. The approach is applicable not only to symmetric but also to asymmetric 2:1 and 1:2 electrolytes solutions in slit shaped nanoscale channels and cylindrical nanocapillaries. In the case of very thick double layers (compared to the channels width) the transport problems are treated numerically.

Applying transverse voltage bias across the channel wall can be used in an attempt to control the transport and such devices are often called “fluidic field effect transistors”. Our model quantifies the effect of the voltage bias on the zeta potential of the channel wall and therefore can be used for prediction of transport and optimization of separations in such fluidic devices.

We show that the conductivity properties of fluidic nanochannels filled with electrolyte solution strongly depend strongly on the channel dimension. As the channel becomes thinner, the migration conductivity contribution monotonically increases while the convective term, due to the electroosmotic flow, passes through a maximum and then decreases. The total conductivity is greater for narrow channels due to the dominance of the migration current transport in this size range. Using electrolytes, that provide divalent counterions to the double layers in the channel, dramatically improves the conductivity even if the overall ionic strength remains the same. Therefore a proper selection of the electrolyte is essential for the performance of a field effect nanofluidic fluidic device. Cylindrical nanocapillaries have better conductivity than parallel slit shaped channels. The transverse voltage bias has a much stronger effect on modulating the wall electrokinetic potential and the double layer for narrow channels that are smaller than the double layer thickness. All these effects need to be taken into account when designing a nanofluidic device for a particular application.

## Introduction

The transport of fluid, current and dissolved analytes in channels of nanometer size presents both fundamental and practical interest. Nanofluidic devices has been successfully used for molecular and biomolecular sensing and analysis.<sup>1-4</sup> A convenient method for

nanochannel fabrication is based on interferometric lithography<sup>5</sup> which was recently used to fabricate channel between 35 and 500 nm for fluidic experiments<sup>4</sup>. A key quantity governing the transport is the potential and charge at the channel wall/solution interface because of the essential importance of the electrokinetic phenomena. The interfacial potential is referred to as  $\zeta$ -potential. Any means for its control and manipulation provide a powerful and convenient tool for governing the transport in the channel. A method for modify the  $\zeta$ -potential, by applying a transverse voltage bias across the channel wall, was suggested more than a decade ago in the pioneering works of Ghowsi and Gale.<sup>6,7</sup> Using this technique Schafoort *et al.*<sup>8</sup> were able to control the magnitude and even the direction of electroosmotic fluid flow in a microfluidic channel. The transport of electric current is also amenable to variations with changing the potential at the wall/solution interface.<sup>9</sup>

Manipulating the  $\zeta$ -potential by applying a voltage bias across the channel wall gives rise to the possibility of creating fluidic “field effect transistor” devices at the micro<sup>6-8, 10-14</sup> and the nanoscale.<sup>9, 15</sup> A particularly interesting work was recently published, demonstrating the viability of this idea for designing a variety of nanofluidic diodes and transistors.<sup>16</sup> The control over the transport of current described in this work<sup>17</sup> was again accomplished by modulating the electric double layer in the channel through the interfacial  $\zeta$ -potential.

At the nanoscale, the channel width might be comparable to the thickness of the electric double layer. The double layer thickness on the other hand depends on the electrolyte concentration. Thus, for electrolyte concentrations ranging between  $10^{-6}$  and  $10^{-2}$  M (symmetric monovalent electrolyte), the respective double layer thickness varies from 300 to 3 nm. If the nanochannel width,  $h$ , is greater than the double layer thickness (at least four times or more) the transport of fluid, electric current and dissolved analytes can be treated analytically for an arbitrarily high value of the  $\zeta$ -potential.<sup>15, 18</sup> Otherwise analytical treatment is possible only for small  $\zeta$ -potential (below 25 mV)<sup>19</sup> where many interesting and important features (like the importance of the electrolyte type) are lost.

This paper first presents a concise theory that allows obtaining analytical expressions for the transport of fluid (electroosmotic flow), ions (electric current) and dissolved charged molecules (analytes) in the case of a weak double layer overlap. Then we will focus on a numerical analysis of the transport of electric current in channels with dimensions of the order or even less than the thickness of the respective electric double layers. We analyze (i) the effect of the channel width (or equivalently the double layer thickness), (ii) the channel shape (comparing parallel slit shaped channels with cylindrical capillaries) and (iii) the role of the electrolyte and more specifically the type of the counterion (monovalent or divalent). While the latter is often overlooked, we show that it has a tremendous impact on the performance of nanofluidic field effect devices. We discuss the particular cases of 1:1 and 2:1 electrolytes. For very narrow channels (relatively to the double layer thickness) the co-ions are unimportant for the conductivity because they are in a negligible concentration in comparison with the counterions.<sup>20</sup> Hence, the conclusions we make for 2:1 electrolytes (where the counterions have two charges and the co-ions just one) will be qualitatively and even semi-quantitatively correct also for symmetric 2:2 electrolytes. It is important to note that our approach is limited to the use of continuum models. For extremely small channels (a few nanometers and below) the molecular structure of the solvent becomes important and the only adequate approaches left are based on molecular dynamics simulations.<sup>21-23</sup> Still there is a wide range of cases where

the nanochannel width might be comparable or even less than the double layer thickness and the continuum theory remains valid.

## Theory

The current in a nanochannel depends on the local concentration of ions. In narrow channels, the local concentration of counterions depends on the electrostatic potential and exceeds that in a bulk solution, which is in thermodynamic equilibrium with the overlapping double layers. This leads to an increase of the conductivity of the electrolyte solution in the channel compared to that in the bulk. The electrostatic potential distribution in a nanochannel filled with electrolyte solution,  $\Psi$ , is given by the Poisson-Boltzmann equation which for binary ( $z_1:z_2$ ) electrolyte reads<sup>24</sup>

$$\nabla^2 \tilde{\Psi} = -\frac{\kappa^2}{z_1 + z_2} \left[ \exp(-z_1 \tilde{\Psi}) - \exp(z_2 \tilde{\Psi}) \right], \tilde{\Psi} = \frac{e\Psi}{kT} \quad (1)$$

where

$$\kappa^2 = \frac{e^2 (z_1^2 n_1 + z_2^2 n_2)}{\varepsilon \varepsilon_0 kT} \quad (2)$$

defines the inverse thickness of the double layer, often referred to as Debye screening parameter.<sup>25</sup>  $e$  is the elementary charge,  $kT$  is the thermal energy,  $\varepsilon$  and  $\varepsilon_0$  are the relative dielectric permittivity (78.25 for water at 25°C) and the dielectric constant of vacuum ( $8.854 \times 10^{-12} \text{ C}^2 \text{ J}^{-1} \text{ m}^{-1}$ ) and  $n_i$  are ionic the number densities. The boundary conditions are:  $\Psi = \zeta$  and the wall and  $\nabla\Psi = 0$  in the center of the channel (symmetry). The second order differential operator in (1) depends on the shape of the channel:  $\nabla^2 = d^2 / dx^2$  for parallel slits and  $\nabla^2 = d^2 / dr^2 + (1/r) d / dr$  for cylindrical capillary. All edge effect at the channel entrance and exit are ignored. The screening parameter  $\kappa$  [see eq (2)] is defined by the electrolyte concentration of a macroscopic bulk reservoir in fluidic contact and thermodynamic equilibrium with the channels. The total conductivity of a fluidic nanochannel consists of migration a term<sup>26</sup>

$$K_{mig} = \frac{j_{mig}}{E} = \frac{e^2}{AkT} \int_A \left\{ z_1^2 D_1 n_1^0 \exp[-z_1 \tilde{\Psi}(r)] + z_2^2 D_2 n_2^0 \exp[-z_2 \tilde{\Psi}(r)] \right\} dA \quad (3)$$

where  $A$  is the area of the channel cross-section, and a convective electro-osmotic term, which is due to the counterion excess (charge density  $\rho_e$ ) in the double layer carried by the electro-osmotic fluid flow

$$K_{eo} = \frac{j_{eo}}{E} = \frac{1}{A} \int_A \rho_e(r) \frac{\varepsilon \varepsilon_0 [\Psi(r) - \zeta]}{\eta} dA \quad (4)$$

where  $j_{mig}$  and  $j_{eo}$  are the respective migration and electroosmotic convective contribution to the total current density due to the applied field  $E$ . The charge density is

$$\rho_e(r) = e \left\{ z_1 n_1^0 \exp[-z_1 \tilde{\Psi}(r)] - z_2 n_2^0 \exp[z_2 \tilde{\Psi}(r)] \right\} \quad (5)$$

$D_i$  are the diffusion coefficients of the ionic species and  $n_i^0$  are their concentrations in the bulk reservoir that is in contact with the channel.  $\eta$  is the solvent viscosity. The fluid flow that leads to the convective transport of ions [see (4)] is given by<sup>26, 27</sup>

$$\eta \nabla^2 v = (\varepsilon \varepsilon_0 \nabla^2 \Psi) E \quad (6)$$

where  $v$  is the velocity profile and  $E$  is the electric field vector. The boundary conditions require that are  $v = 0$  and  $\Psi = \zeta$  at the shear plane and symmetric in the center of the channel. Then the solution for the fluid flow velocity is

$$v(r) = \frac{\varepsilon \varepsilon_0}{\eta} [\Psi(r) - \zeta] \quad (7)$$

[cf. eq (4)].

The effect of an external voltage bias, applied across the channel wall, on the  $\zeta$ -potential and, hence, the on double layer is given by<sup>15</sup>

$$\Delta\zeta = \Phi_b - \left[ \zeta_0 + \frac{\sigma_0 (\zeta_0 + \Delta\zeta) \delta}{\varepsilon_\delta \varepsilon_0} \right] \quad (8)$$

where  $\Delta\zeta$  is the shift in the interfacial potential (originally equal to  $\zeta_0$ ),  $\sigma_0$  is the surface charge ( $\sigma_0 = -\varepsilon \varepsilon_0 \nabla \Psi|_{wall}$ ),  $\delta$  and  $\varepsilon_\delta$  are the thickness and the relative dielectric permittivity of the channel wall.

The computational procedure includes the following steps: (i) determination of the electrostatic potential distribution in the channel by numerically solving (1) assuming  $\Psi = \zeta$  at the channel wall and symmetry in the center; (ii) the migration conductivity is calculated by numerical integration of eq (3); (iii) the convective contribution to the conductivity is obtained using eq (4) together with (5); (iv) the effect of the transverse voltage bias to modulate the double layer in a field effect applications is computed from eq (8). The migration and convective electroosmotic contributions are presented separately in order to better compare their importance and also because they depend very differently on the relative (with respect to the double layer) width of the nanochannel.

## Results and Discussion

Our theoretical analysis for the moderately thin electrical double layer employs the nonlinear superposition approximation that the total potential in a channel with weakly overlapping double layers is<sup>20, 24, 27, 38, 39</sup>

$$\Psi(x) = \Psi_1(x) + \Psi_1(h-x) \quad (9)$$

where  $\Psi_1$  is the potential of a single double layer. Eq. (9) is a very good approximation for not very thin channels of  $\kappa h \geq 4$ ,<sup>20, 24, 38-40</sup> where double layers only weakly overlap and arbitrarily high  $\zeta$ -potentials. The single flat double layer potential for symmetric electrolyte reads

$$\tilde{\Psi}_1(x) = \frac{4}{z} \arctan h \left[ \tanh\left(\frac{z\tilde{\zeta}}{4}\right) \exp(-\kappa x) \right] = 2 \ln \left[ \frac{1 + \tanh\left(\frac{z\tilde{\zeta}}{4}\right) \exp(-\kappa x)}{1 - \tanh\left(\frac{z\tilde{\zeta}}{4}\right) \exp(-\kappa x)} \right] \quad (10)$$

To obtain potential distribution for asymmetric 2:1 and 1:2 electrolyte, following functions have to be define<sup>24, 41, 42</sup>

$$f_1(\tilde{\Psi}_1) = \ln \left[ \frac{2 \exp(\tilde{\Psi}_1) + 1}{3} \right], |z_1| = 2, |z_2| = 1, \text{ and } f_2(\tilde{\Psi}_1) = \ln \left[ \frac{3}{2 \exp(-\tilde{\Psi}_1) + 1} \right], |z_1| = 1, |z_2| = 2, \quad (11)$$

The function  $f_{21}$  and  $f_{12}$  are obtained from the modified Poisson-Boltzmann equation for a single double layer

$$\frac{d^2 f_i}{dx^2} = \kappa^2 \sinh(f_i), \quad i = 21 \text{ or } 12. \quad (12)$$

The solution of eq. (12) with the boundary conditions  $\tilde{\Psi}_1(0) = \tilde{\Psi}_0$  and  $\tilde{\Psi}_1(\infty) = 0$  becomes

$$f_i(\tilde{\Psi}_1) = 4 \arctan h \left\{ \tanh \left[ \frac{f_i(\tilde{\Psi}_0)}{4} \right] \exp(-\kappa x) \right\}, \quad i = 21 \text{ or } 12 \quad (13)$$

The potential distributions can be easily derived from equation (13), as well as the potential of a slit-shaped nanochannel of width  $h$ . This nonlinear superposition approximation allows us to calculate the electroosmotic flow, electric current and solute flux analytically for symmetric and asymmetric electrolyte.<sup>15</sup>

Figure 1a shows the dependence of the relative migration conductivity ( $\bar{K}_{mig} = K_{mig} / K_{mig}^0$ ) for a parallel slit-shaped fluidic nanochannel with dimensionless width  $\kappa h$  ( $h$  being the dimensional channel width).  $K_{mig}^0$  is the conductivity of a bulk electrolyte solution that is in thermodynamic equilibrium with the channel. Hence, the results presented hereafter show the relative conductivity in the channels with respect to that of the bulk solution (reservoir) that is in thermodynamic equilibrium with double layers,  $K_{mig}^0$ . The data shown in Figure 1 are for a solution of symmetric 1:1 electrolyte (KCl). The diffusion coefficients of  $K^+$  and  $Cl^-$ , necessary for calculating the migration conductivity, are both equal to  $2 \times 10^{-9} \text{ m}^2/\text{s}$ .<sup>28</sup> The different curves correspond to different wall/solution electrokinetic  $\zeta$ -potentials starting from  $\tilde{\zeta} = e\zeta / kT = -1$  ( $\cong -26 \text{ mV}$ , lower curve) to  $\tilde{\zeta} = -4$  ( $\cong -104 \text{ mV}$ , upper curve). The intermediate plots are for  $\tilde{\zeta} = -2$  and  $\tilde{\zeta} = -3$ , respectively. The choice of negative surface potential is because most materials, used for channels fabrication, are negatively charged under the common experimental condition (for example  $\text{SiO}_2$  or glass at neutral pH). This, however, does not limit the general validity of our considerations and conclusions. The relative conductivity decreases with the width of the channel,  $h$ , and eventually approaches that in the bulk for  $h \rightarrow \infty$ . Decreasing the electrolyte concentration [or the parameter  $\kappa$ , see eq (2)] has the same effect of increasing the relative conductivity. However, one should keep in mind that in this case the bulk conductivity,  $K_{mig}^0$ , also decreases. Hence the curves in Figure 1 can be obtained by two different methods. The first one is by bringing the walls closer, which leads to an increase of the channel conductivity, while that in the bulk reservoir remains unchanged. The second method is by decreasing the ionic strength of the solution which decreases the conductivity both in the channel and in the bulk. The rate of conductivity decrease in the channel, however, is lower than that in the bulk.

The convective electroosmotic contribution ( $\bar{K}_{eo} = K_{eo} / K_{mig}$ ) behaves rather differently (see Figure 1b). The curves again correspond to different  $\zeta$ -potential starting from  $\tilde{\zeta} = e\zeta / kT = -1$  ( $\cong -26 \text{ mV}$ , lower curve) to  $\tilde{\zeta} = -4$  ( $\cong -104 \text{ mV}$ , upper curve). For large

channels the convective electroosmotic term equals the charge density in two infinitely separated double layers multiplied by the electroosmotic fluid flow. As the walls come closer the electroosmotic conductivity increases due to the increase of the counterion density in the channel  $\rho_e(r)$  as the double layers overlap [see eq (4)]. At the same time, however, the difference  $[\Psi(r) - \zeta]$  becomes smaller. Thus after passing through a maximum, the electroosmotic conductivity rapidly decreases and tends to zero at  $\kappa h \rightarrow 0$ . The maxima in  $\bar{K}_{eo}$  occur at  $\kappa h \cong 0.6$  for  $\tilde{\zeta} = -4$ , at  $\kappa h \cong 1.0$  for  $\tilde{\zeta} = -3$ ,  $\kappa h \cong 1.5$  for  $\tilde{\zeta} = -2$  and at  $\kappa h \cong 2.0$  for  $\tilde{\zeta} = -1$ . At  $\kappa h \rightarrow 0$  the potential in the channel approaches a constant value (equal to  $\zeta$ ) everywhere. This means that the fluid flow ceases [see also Refs. <sup>29, 30</sup>] and no ions are carried by means of convection. Also in the absence of double layers (e.g. when  $\zeta = 0$ ) the electroosmotic term is identically equal to zero.

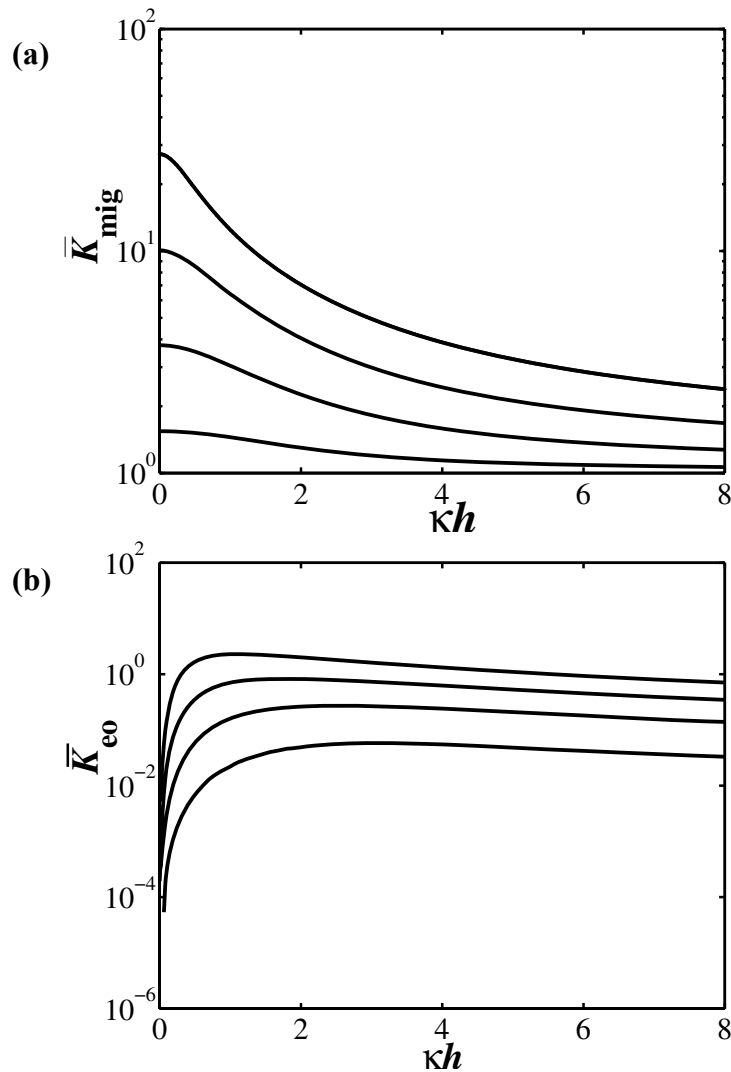
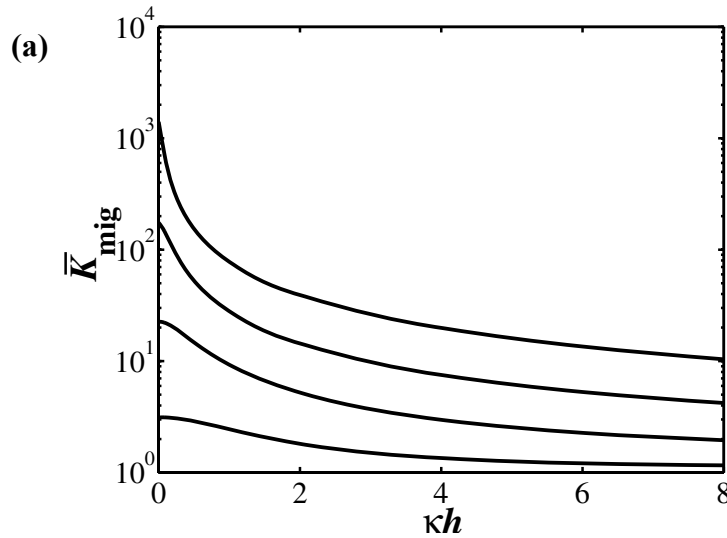


Figure 1. Conductivity of parallel slit shaped fluidic channel filled with KCl solution vs width: (a) migration contribution and (b) convective contribution. The different curves correspond to (top to bottom)  $\tilde{\zeta} = -4$ ,  $\tilde{\zeta} = -3$ ,  $\tilde{\zeta} = -2$  and  $\tilde{\zeta} = -1$ .

Since the migration (Figure 1a) and electroosmotic (Figure 1b) conductivity terms depend very differently on the channel width (i.e. on  $\kappa h$ ), their relative importance changes with  $\kappa h$ . The migration term decays more rapidly than the electroosmotic term as  $\kappa h$  increases. For  $\tilde{\zeta} = -4$  (-104 mV) and  $\kappa h \cong 4$ , the electroosmotic term corresponds to 25% of the overall conductivity of the nanochannel (maximum value for these conditions). The relative importance of the electroosmotic with respect to the total conductivity  $K_{eo} / (K_{mig} + K_{eo})$  decreases for lower magnitude of the  $\zeta$ -potentials and the maximum and shifts to larger values of  $\kappa h$ .

Increasing the charge number of the counterions has a very strong impact on the conductivity of the nanochannel. Using an asymmetric 2:1 electrolyte (e.g.,  $MgCl_2$ ) increases substantially both the migration and electroosmotic terms (see Figure 2). This is due to the fact that the divalent counterions are much more efficient charge carriers and also tend to accumulate in greater concentrations in the double layers because of the stronger electrostatic attraction. The diffusion coefficients used to calculate the migration term were  $7 \times 10^{-10} \text{ m}^2/\text{s}$  and  $2 \times 10^{-9} \text{ m}^2/\text{s}$  for  $Mg^{2+}$  and  $Cl^-$  respectively. While the values of the migration and electroosmotic conductivities (see Figure 2a and 2b) are much greater, the trend with varying the dimensionless channel width  $\kappa h$  is qualitatively similar to that for symmetric monovalent electrolyte. The maxima in the  $K_{eo}$  curves are more distinct and occur at smaller channel widths ( $\kappa h \cong 0.1$  for  $\tilde{\zeta} = -4$ , at  $\kappa h \cong 0.4$  for  $\tilde{\zeta} = -3$ ,  $\kappa h \cong 1.0$  for  $\tilde{\zeta} = -2$  and at  $\kappa h \cong 2.0$  for  $\tilde{\zeta} = -1$ ). The relative importance of the electroosmotic conductivity contribution again depends on the dimensionless channel width and wall/solution  $\zeta$ -potential. For  $\tilde{\zeta} = -4$  the maximum electroosmotic contribution is again about 25% of the total channel conductivity but it corresponds to smaller channels ( $\kappa h \cong 1$ ). Again, the relative importance of the electroosmotic conductivity  $K_{eo} / (K_{mig} + K_{eo})$  decreases for lower magnitude of the  $\zeta$ -potentials and the maximum and shifts to larger values of  $\kappa h$ .



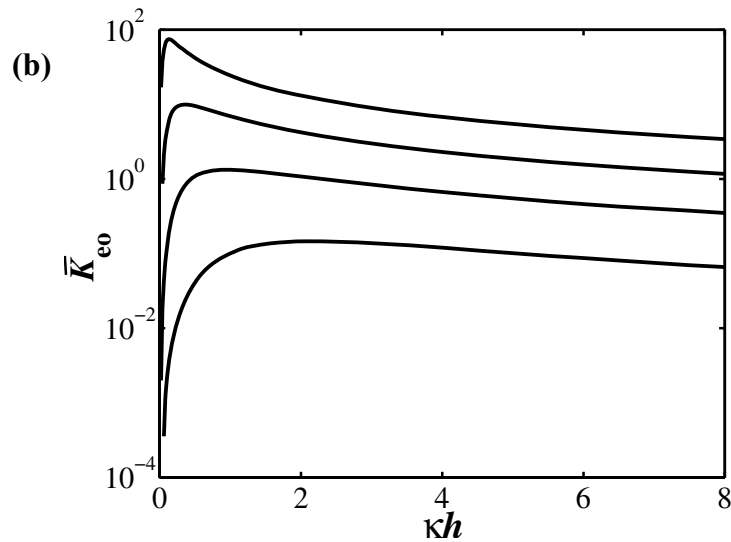
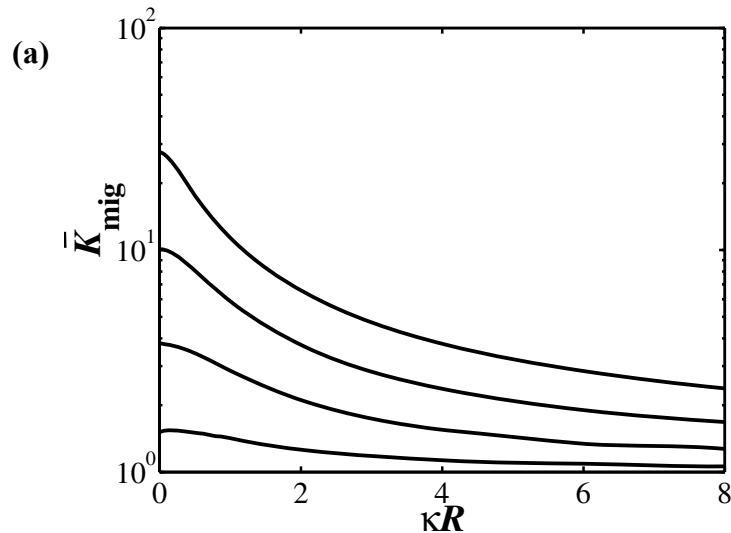


Figure 2. Conductivity of parallel slit shaped fluidic channel filled with  $\text{MgCl}_2$  solution vs width: (a) migration contribution and (b) convective contribution. The different curves correspond to (top to bottom)  $\tilde{\zeta} = -4$ ,  $\tilde{\zeta} = -3$ ,  $\tilde{\zeta} = -2$  and  $\tilde{\zeta} = -1$

Figure 3 represents the results for the migration and electroosmotic convective contribution to the conductivity for KCl in a cylindrical capillary as a function of the dimensionless radius  $\kappa R$ . Our calculation is similar to that of Morrison and Osterle who presented data for the total conductivity [i.e.  $(K_{mig} + K_{eo})K_{mig}^0$ ] of a capillary filled with water.<sup>31</sup> The shape of the conductivity curve in their paper is due to the superposition of migration and electroosmotic convective contributions.



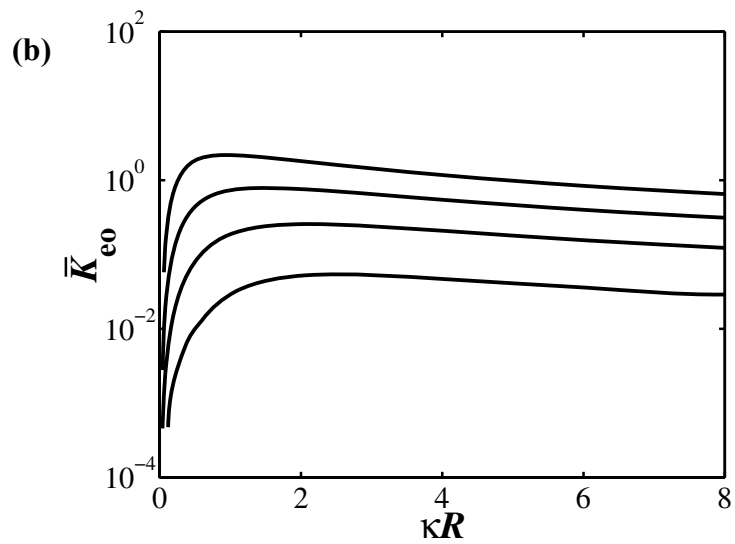
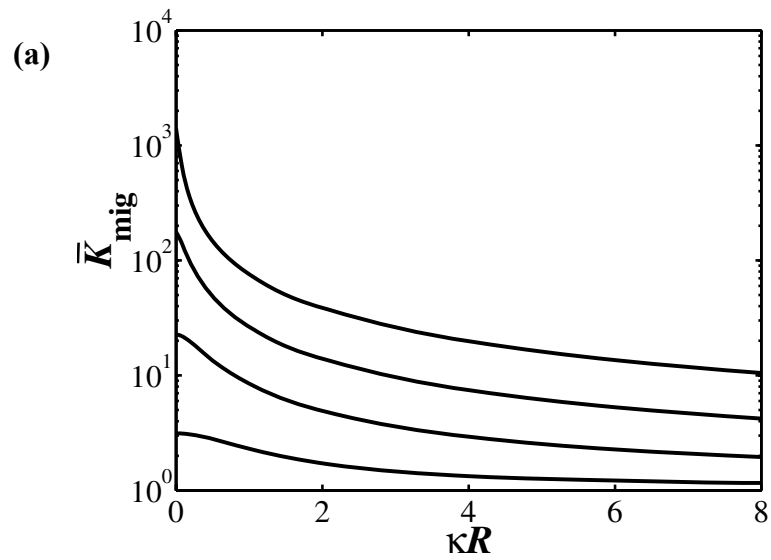


Figure 3. Conductivity of cylindrically shaped fluidic channel filled with KCl solution vs radius: (a) migration contribution and (b) convective contribution. The different curves correspond to (top to bottom)  $\tilde{\zeta} = -4$ ,  $\tilde{\zeta} = -3$ ,  $\tilde{\zeta} = -2$  and  $\tilde{\zeta} = -1$ .



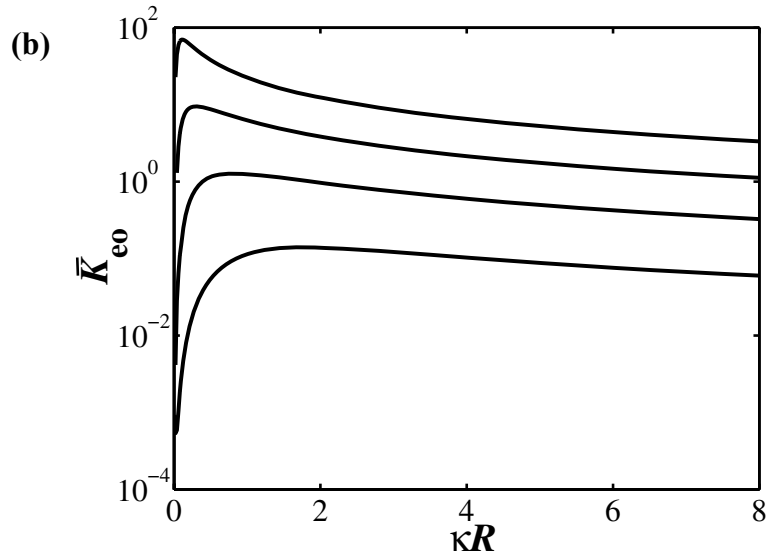


Figure 4. Conductivity of cylindrically shaped fluidic channel filled with  $\text{MgCl}_2$  solution vs radius: (a) migration contribution and (b) convective contribution. The different curves correspond to (top to bottom)  $\tilde{\zeta} = -4$ ,  $\tilde{\zeta} = -3$ ,  $\tilde{\zeta} = -2$  and  $\tilde{\zeta} = -1$ .

The rate of decrease of both migration and convective electroosmotic terms relative to that in the bulk, presented in Figure 3, is lower than the corresponding rates of decrease in parallel slits (see Figure 1). The channel dimension in this case is given in terms of the radius and the total width (diameter) is actually two times larger. Hence, channels with curved (cylindrical) walls are more efficient in conducting electrical current than parallel slits. The physical reason for this fact is that the electrostatic potential in a cylindrical channel decays less from the wall toward the center than it does in a parallel slit-shaped channel due to the additional term  $(1/r) d/dr$  in the second order differential operator [see the discussion after eq (2) above]. Same is valid for the case of asymmetric 2:1 electrolyte (see Figure 4). Therefore a cylindrical shape is preferable if better conductivity is intended. In fact a cylindrical channel with divalent counterions in the wall double layer is the best candidate if one aims for high conductivity at given ionic strength.

The transport of fluid and current in a cylindrical capillary was treated analytically by Rice and Whitehead<sup>19</sup> assuming low  $\zeta$ -potential ( $|\tilde{\zeta}| < 1$ ). This allows the linearization of (1) and hence its analytical solution. By doing that however, the effect of the electrolyte type (counterion charge number) is lost and the potential distribution depends only on the screening parameter  $\kappa$ . As we showed above, however, using divalent instead of monovalent counterions increases dramatically the nanochannel conductivity even if the ionic strength of the solution (or  $\kappa$ ) remains the same, which is due to the nonlinearity of the Poisson Boltzmann equation (1). This means that channels with low surface potential are less interesting from the perspective of design, optimization and control of nanofluidic field effect transistor devices. An alternative analytical model for the electroosmotic fluid flow for moderately thin double layer was recently developed using the matched asymptotic expansions approach.<sup>18</sup> The model is valid for arbitrarily high potentials but is not applicable to systems with thick double layers.

The above results imply that there is an important qualitative difference between symmetric and asymmetric electrolyte solution in nanochannels. The dependence of the channel conductivity filled with symmetric electrolyte (e.g., KCl) shows a symmetric dependence on the value and sign of the electrokinetic  $\zeta$ -potential at the wall. Thus the channel conductivities for equal in magnitude but opposite in sign potential are identical – see Figure 5a. Switching the sign of the  $\zeta$ -potential leads to replacing the counterions with others with an opposite sign. In the case of KCl this means that  $K^+$  would be replaced by  $Cl^-$  or vice versa. The total concentration of ions in the channel however, would remain unchanged. Since the ionic diffusion coefficients, and hence the mobilities for  $K^+$  and  $Cl^-$  are the same, the curves shown in Figure 5a are perfectly symmetrical with respect to the vertical axis. In the case of asymmetric electrolyte (e.g.,  $MgCl_2$ ) however the situation is very different. For the same ionic strengths, the conductivities for negative  $\zeta$ -potentials are much higher than those for positive  $\zeta$ -potentials (if the absolute value remains the same). The difference is rather substantial, more than an order of magnitude (Figure 5b). Hence, this effect can be used in nanofluidic devices to control the direction of current transport by manipulating the sign of the electrokinetic  $\zeta$ -potential at the channel wall. Examples for directionality in the current transport in fluidic devices has been suggested and studied by other authors<sup>17, 32-37</sup> using different physical principles. Karnik *et al.*<sup>17</sup> approach is based on controlling the overall amount of ions in the channel by modulating the  $\zeta$ -potential. Increasing or decreasing this potential changes the number of ions in the channel and hence the observed conductivity (see Figure 5a). Siwy *et al.* and Woermann on the other rely on the asymmetric conical shape of the channel to obtain directionality in the current transport. A particularly interesting design for a nanofluidic diode was suggested by Daiguchi *et al.*<sup>16</sup> Their design is based on the fabrication of channels with walls that have oppositely charged regions next to each other, which is not trivial from fabrication viewpoint although it is rather elegant. Our results (shown in Figure 5b) suggest that using an asymmetric electrolyte (which is not a problem in most cases) provides an additional opportunity to control the current transport and obtain a diode-like conductivity.

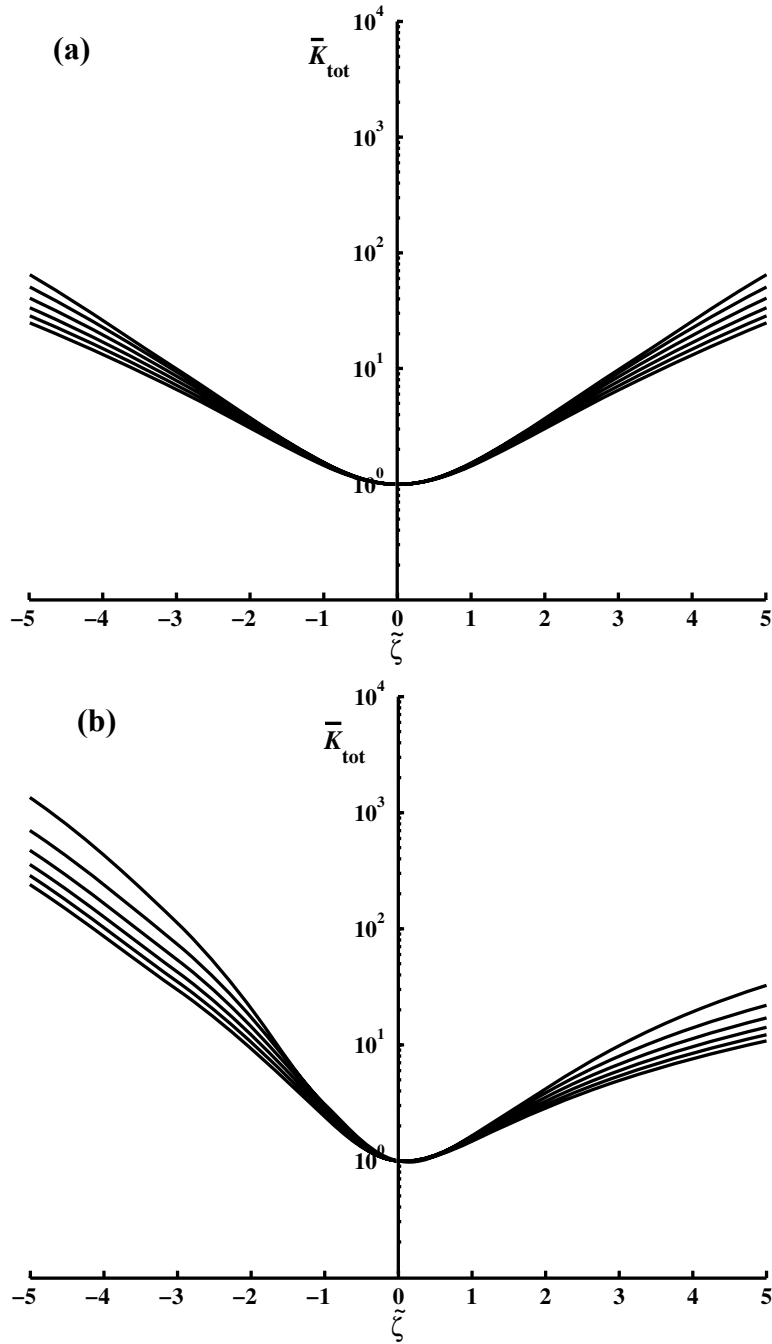
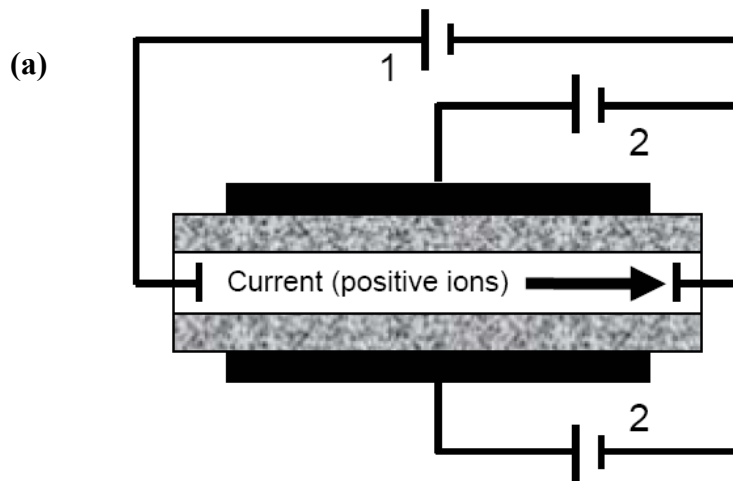


Figure 5. Total relative conductivity in a slit-shaped nanochannel  $\bar{K}_{tot} = \bar{K}_{mig} + \bar{K}_{eo}$  vs. the electrokinetic  $\zeta$ -potential. The different curves (top to bottom) correspond to  $\kappa h = 0.2, 0.4, 0.6, 0.8, 1.0, 1.2$ . (a) symmetric electrolyte (KCl); (b) asymmetric electrolyte (MgCl<sub>2</sub>).

All the above considerations and discussions are based on an assumption that there is no significant adsorption of divalent counterions at the channel walls. Ionic adsorption could immobilize part of the counterions and more importantly decrease the electrokinetic  $\zeta$ -potential. In this case both the conductivity and electroosmotic fluid flow could be less than in the case of monovalent electrolyte. Therefore, at high ionic strengths and in the present of strongly

adsorbing divalent counterions, the  $\zeta$ -potential could be reduced thus reducing the transport of current and fluid.

In order to have a working fluidic field effect transistor device one needs to modulate the double layer in the channel.<sup>6-15, 17</sup> This can be done by applying voltage at the channel wall via a third electrode [see Refs.<sup>6-17</sup> for detailed description of the design]. If the wall is mostly insulating (in comparison with the electrolyte solution) the induced field propagates across a dielectric continuum and its effect on the wall/solution  $\zeta$ -potential is given by eq (8).<sup>15</sup> Figure 6a shows a sketch of a nanofluidic device with modulated  $\zeta$ -potential using a voltage applied across the channel walls. Figure 6b shows a plot of the bias voltage necessary obtain certain change in the  $\zeta$ -potential (i.e.  $\Delta\zeta$ ) against the dimensionless channel width  $\kappa h$ . The results are for a parallel slit shaped channel filled with KCl. The curves correspond to different target  $\Delta\zeta$  starting from  $\Delta\zeta = 1$ , lower curve and ending with  $\Delta\zeta = 5$ , top curve. The calculations are for  $\kappa\delta = 2$  and  $\epsilon/\epsilon_\delta = 78.25/2.1 = 37.26$ . The important conclusion from this Figure is that the wall/solution potential is much less responsive to the applied transverse bias for  $\kappa h \geq 1$ . The response of the  $\zeta$ -potential to external voltage biasing is weaker if the counterions in the double layer are divalent because of their greater charge screening effect.<sup>15</sup> This means that while the presence of divalent counterions in the electrolyte solution increases the channel conductivity (see above), its responsiveness to voltage modulation decreases. The effect can be compensated for by decreasing the thickness of the wall layer or its dielectric constant [selecting a different material – see eq (8)].



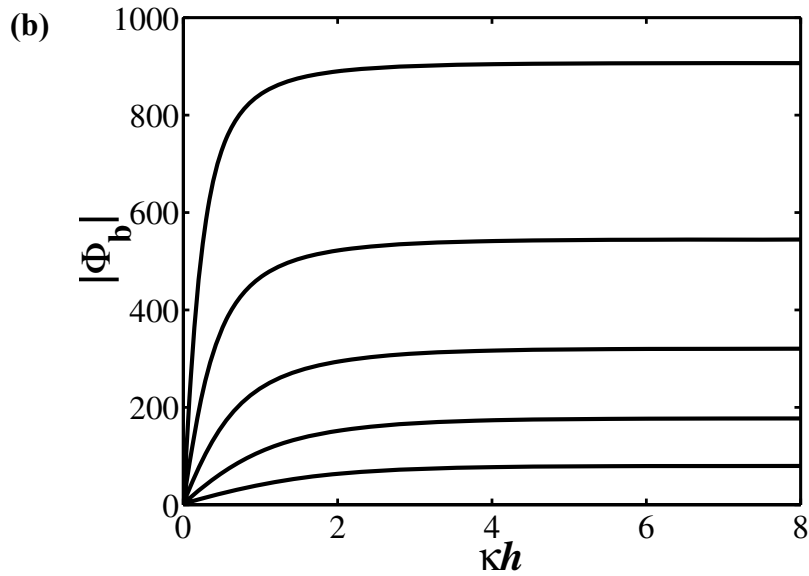


Figure 6. Transverse voltage bias necessary to obtain given  $\Delta\tilde{\zeta}$  [see eq (8)] vs channel width. (a) a sketch of a nanofluidic channel with modulated  $\zeta$ -potential. 1- current driving source, 2- potential modulation source. (b) results for the  $\zeta$ -potential modulation for slit shaped channel. The different curves correspond to (top to bottom):  $|\Delta\tilde{\zeta}| = 5$ ,  $|\Delta\tilde{\zeta}| = 4$ ,  $|\Delta\tilde{\zeta}| = 3$ ,  $|\Delta\tilde{\zeta}| = 2$ , and  $|\Delta\tilde{\zeta}| = 1$ .

### Conclusions

In summary, the conductivity properties of fluidic nanochannels filled with electrolyte solution depend strongly on the channel dimension. As the channel becomes thinner, the migration contribution monotonically increases while the convective term due to the electroosmotic flow passes through a maximum and then sharply decreases. Still, the total conductivity is greater for narrow channels due to the dominance of the migration current transport in this size range. Using electrolytes, that provide divalent counterions to the double layers in the channel, dramatically improves the conductivity even if the overall ionic strength (i.e.  $\kappa$ ) remains the same. Therefore a proper selection of the electrolyte is essential for the performance of a field effect fluidic device. Cylindrical nanocapillaries have better conductivity than parallel slit shaped channels. The transverse voltage bias has a much stronger effect on modulating the  $\zeta$ -potential and the double layer for narrow channels ( $\kappa h < 1$ ). The use of divalent counterions, however, inhibits the response to the external bias.<sup>15</sup> All these effects need to be taken into account when designing a nanofluidic device for a particular application.

*Acknowledgements:* This work has been supported by the NSF/NIRT Program (Grant CTS 0404124)

## Reference

- (1) Han, J.; Craighead, H. G. (2000) *Science*, 288, 1026.
- (2) Saleh, O. A.; Sohn, L. L. (2003) *Nano Lett.*, 3, 37.
- (3) Chang, H.; Kosari, F.; Andreadakis, G.; Alam, M. A.; Vasmatzis, G.; Bashir, R. (2004) *NanoLett.*, 4, 1551.
- (4) Garcia, A.; Ista, L. K.; Petsev, D. N.; O'Brien, M. J.; Bisong, P.; Mammoli, A. A.; Brueck, S. R. J.; Lopez, G. P. (2005) *Lab on a Chip*, 5, 11, 1271-1276.
- (5) O'Brien, M. J.; Bisong, P.; Ista, L. K.; Rabinovich, E. M.; Garcia, A. L.; Sibbett, S. S.; Lopez, G. P.; Brueck, S. R. J. (2003) *J. Vac. Sci. Technol. B*, 21, 2941.
- (6) Ghowsi, K.; Gale, R. J. (1991) *J. Chromatography*, 559, 95.
- (7) Ghowsi, K.; Gale, R. J. (1991) *Am. Laboratory*, 23, 17.
- (8) Schafoort, R. B. M.; Schlautmann, S.; Hendrikse, J.; Berg, A. v. d. (1999) *Science*, 286, 942.
- (9) Daiguji, H.; Yang, P.; Majumdar, A. (2004) *Nano Lett.*, 4, 137.
- (10) Lee, C. S.; Blanchard, W. C.; Wu, C.-T. (1990) *Anal. Chem.* 62, 1550.
- (11) Hayes, M. A.; Ewing, A. G. (1992) *Anal. Chem.*, 64, 512.
- (12) Hayes, M. A.; Kheterpal, I.; Ewing, A. G. (1993) *Anal. Chem.* 65, 2010.
- (13) Polson, N. A.; Hayes, M. (2000) *Anal. Chem.* 72, 1088.
- (14) Buch, J. S.; Wang, P.-C.; DeVoe, D. L.; Lee, C. S. (2001) *Electrophoresis* 22, 3902.
- (15) Petsev, D. N. (2005) *J. Chem. Phys.* 123, 244907.
- (16) Daiguji, H.; Oka, Y.; Shirono, K. (2005) *Nano Lett.* 5, 2274.
- (17) Karnik, R.; Fan, R.; Yue, M.; Li, D.; Yang, P.; Majumdar, A. (2005) *Nano Lett.* 5, 943.
- (18) Petsev, D. N.; Lopez, G. P. (2006) *J. Colloid Interface Sci.* 294, 492.
- (19) Rice, C. L.; Whitehead, R. (1965) *J. Phys. Chem.* 69, 4017.
- (20) Verwey, E. J. W.; Overbeek, J. T. G. (1948) *Theory and Stability of Lyophobic Colloids*; Elsevier: Amsterdam.
- (21) Qiao, R.; Aluru, N. R. (2003) *J. Chem. Phys.* 118, 4692.
- (22) Thompson, A. P. (2003) *J. Chem. Phys.* 119, 7503.
- (23) Karniadakis, G.; Beskok, A.; Aluru, N. (2005) *Microflows and Nanoflows*; Springer: New York.
- (24) Derjaguin, B. V.; Churaev, N. V.; Muller, V. M. (1987) *Surface Forces*; Plenum: New York.
- (25) Debye, P. (1923) *Phys. Ztschr.* 24, 185.
- (26) Dukhin, S. S.; Derjaguin, B. V. (1974) In *Surface and Colloid Science*; Matijevic, E., Ed.; Wiley Interscience: New York, Vol. 7, pp 49.
- (27) Hunter, R. J. (1981) *Zeta Potential in Colloid Science*; Academic Press: New York.
- (28) Samson, E.; Marchand, J.; Snyder, K. A. (2003) *Materials and Structures* 36, 156.
- (29) Levine, S.; Marriot, J. R.; Robinson, K. (1975) *J. Chem. Soc. Faraday Trans II* 71, 1.
- (30) Levine, S.; Marriot, J. R.; Neale, G.; Epstein, N. (1975) *J. Colloid Interface Sci.* 52, 136.
- (31) Morrison, F. A.; Osterle, J. F. (1965) *J. Chem. Phys.* 43, 2111.
- (32) Siwy, Z.; Fulinski, A. (2002) *Phys. Rev. Lett.* 89, 198103.
- (33) Siwy, Z.; Dobrev, D.; Neumann, R.; Trautmann, C.; Voss, K. (2003) *Appl. Phys. A* 76, 781
- (34) Siwy, Z.; Fulinski, A. (2004) *Am. J. Phys.*, 72, 567.
- (35) Siwy, Z.; Heins, E.; Harrell, C. C.; Kohli, P.; Martin, C. R. (2004) *J. Amer. Chem. Soc.* 126, 10850.
- (36) Siwy, Z. (2006) *Adv. Funct. Mater.* 16, 735.

- (37) Woermann, D. (2003) *Phys. Chem. Chem. Phys.* 5, 1853.
- (38) Derjaguin B.V. (1989) *Theory of Stability of Colloids and Thin Films* (Plenum, New York)
- (39) Overbeek J.Th.G. (1952) in *Colloid Science*, edited by H.R. Kruyt (Elsevier, Amsterdam) 1, 245, 302
- (40) Russel W.B.; Saville D.A.; Schowalter W.R. (1989) *Colloidal Dispersions* (Cambridge University Press, Cambridge)
- (41) Muller, V.M. (1976) *Colloid J. USSR* 38, 704
- (42) Abraham-Shrauner B. (1973) *J. Colloid Interface Sci.* 44, 77; Abraham-Shrauner B. (1975) *J. Colloid Interface Sci.* 53, 496; Marmur A. (1979) *J. Colloid Interface Sci.* 71, 610